Pressure Normal Derivative Extraction for Arbitrarily Shaped Surfaces

Endrias G. Asgedom ,Okwudili Chuks Orji, Walter Söllner, PGS*

SUMMARY

The normal derivative of the pressure field at a recording surface has proven to be very useful information for deghosting and extrapolation of marine seismic data. The Kirchhoff-Helmholtz integral with the Green's function source outside a (source free) closed surface relates the pressure field at the surface with its normal derivative. However, extracting the normal derivative of the pressure field from the recorded pressure is not a trivial task. This is because; first, the Green's function containing the scattering information from a spatio-temporally varying sea surface must be known; and second, the signal-to-noise ratio of pressure measurement at notch frequencies are notoriously poor. In this paper, we present a method based on the Kirchhoff-Helmholtz integral equation for extracting the normal derivative of the pressure field (away from notch locations) for any arbitrarily shaped sea surfaces. The validity of the method is demonstrated using both synthetic and field datasets obtained using a dual-sensor streamer.

INTRODUCTION

Prediction of the total pressure field (or separation of wavefield) at a given location different from the surface where the wavefield was recorded based on the Kirchhoff-Helmholtz integral requires the pressure wavefield and its normal derivative at the recording surface as input. However, the pressure field and its normal derivative at the recording surface are not prescribed independently (Copley, 1968; Schenck, 1968; Veronesi and Maynard, 1988; Amundsen, 1994). Thus, provided that we are away from the notch locations and know the shape of the sea surface, the normal derivate of the pressure field can be determined from the recorded pressure field.

Amundsen et al. (1995), presented a method based on the Kirchhoff-Helmholtz integral for extracting the normal component of the particle velocity at the recording surface for the case of a flat sea surface. In this paper, we generalize this idea for any arbitrarily shaped sea surface and extract the normal derivative of the pressure field. Information about the shape of the sea surface at any given space and time can be obtained employing dual sensor data (Orji et al., 2010, 2012) or from very low frequency pressure recordings (Laws and Kragh, 2006). The generalized scheme for extracting the normal derivative of the pressure field is implemented and validated using rough sea synthetic data and deep water field data from offshore Brazil.

THEORY

Consider a mono-frequent pressure wavefield, $P(\mathbf{r_r},\mathbf{r_s})$ generated by a source at $\mathbf{r_s}$ and recorded at a receiver location $\mathbf{r_r}$. This pressure field satisfies the *homogenous* Helmholtz wave equation inside a given *source free* closed surface S. In marine seismic acquisition, a suitable closed surface that has the recording surface S_r as part of the closed surface is often selected (cf. Fig. 1). Now, selecting a causal Green's function, *with the same medium parameters as the pressure field within and on the surface S* , the Kirchhoff-Helmholtz integral can be written as (Morse and Feshbach, 1953)

$$\alpha P(\mathbf{r}) = \int_{S_r}\left[G(\mathbf{r_r},\mathbf{r})\frac{\partial P(\mathbf{r_r},\mathbf{r_s})}{\partial n} - P(\mathbf{r_r},\mathbf{r_s})\frac{\partial G(\mathbf{r_r},\mathbf{r})}{\partial n}\right]dS_r\ , \tag{1}$$

where

$$\alpha = \begin{cases} 1 & \text{if } \mathbf{r} \text{ is inside S} \\ 0 & \text{if } \mathbf{r} \text{ is outside S}\ , \end{cases}$$

with $\mathbf{n}$ denoting normal to the surface. Here, we have employed the fact that the closed surface S can be decomposed into the recording surface S_r and a hemispherical surface S_R. By assuming the surface S_R is located at infinity, its contribution to the Kirchhoff-Helmoltz integral becomes zero as a result of Sommerfeld radiation condition (Sommerfeld, 1954).

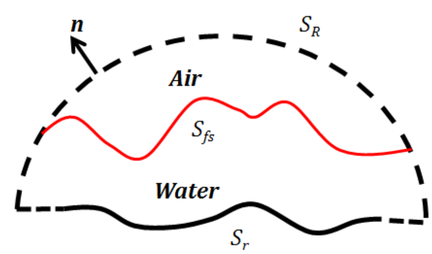

Figure 1: Problem geometry with the closed surface S comprising the recording surface S_r and a hemispherical surface S_R. S_{fs} represents the free surface.

Relationship Between Pressure and its Normal Derivative at the Recording Surface

If the Green's function source location lies below the recording surface ($\mathbf{r} = \mathbf{r_r} + \varepsilon$, with ε being some distance in the normal direction) and replacing the integration with that of quadrature summation, Eq. 1 redues to

$$\mathbf{D}_{qj}P^j = \mathbf{M}_{qj}\frac{\partial P^j}{\partial n}\ , \tag{2}$$

$\mathbf{D}$ and $\mathbf{M}$ are the *dipole* and *monopole* matrices, respectively. Moreover, q is the Green's function source index and j is the receiver location index. Here summation is implied over all repeated indices. Eq. 2 is the basis for extracting the normal derivative of the pressure field from the measured pressure. It is pertinent to note that selecting a very small or very large ε results in numerical artifacts (Amundsen et al., 1995).

DOI http://dx.doi.org/10.1190/segam2014-0480.1

Computing the Green's Function and its Normal Derivative

Until now we have assumed that the Green's function and its normal derivative are known. When the sea surface is flat, the Green's function and its normal derivative can be obtained using *the method of images* (Morse and Feshbach, 1953). However, when the sea surface varies in shape (or does not correspond to separable coordinate system geometries), the Green's function can be determined based on the Kirchhoff-Helmholtz integral equation with the *actual source inside* the closed surface. Consider now a closed surface that includes the free surface (cf. Fig. 2) and replace the actual source with a Dirac delta pulse $\delta(\mathbf{r}' - \mathbf{r})$. Invoking Sommerfeld radiation condition over S_R and imposing the free surface boundary condition over S_{fs} ($G(\mathbf{r}')|_{\mathbf{r^s}} = 0$, where $\mathbf{r^s}$ is the observation point on S_{fs}); the Kirchhoff-Helmhotlz integral gives

$$\alpha G(\mathbf{r}') = G^0(\mathbf{r},\mathbf{r}') - \int_{S_{fs}} G^0(\mathbf{r^s},\mathbf{r}') \frac{\partial G(\mathbf{r^s},\mathbf{r})}{\partial n_1} dS_{fs} \,, \quad (3)$$

where

$$\alpha = \begin{cases} 1 & \text{if } \mathbf{r}' \text{ is inside S} \\ 0 & \text{if } \mathbf{r}' \text{ is outside S} \,, \end{cases}$$

G^0 is the free space Green's function and where $\mathbf{n_1}$ is the normal at the surface. Here, note that the Green's function $G(\mathbf{r}')$ represents the pressure field as a result of two sources; first the actual Dirac delta pulse and second the free surface. The strategy for computing the Green's function and its normal derivative at the streamer location based on Eq. 3 is summarized as follows:

- I Selecting $\alpha = 1$ in Eq. 3 and taking the limit when $\mathbf{r}'$ approaches the free surface and also using the free surface boundary condition ($G(\mathbf{r}')|_{\mathbf{r^s}} = 0$), calculate the normal derivative of the Green's function at the free surface.
- II Inserting back the computed normal derivative of the Green's function at the free surface from (*I*) and solving Eq. 3 for $\alpha = 1$ and $\mathbf{r}' = \mathbf{r_r}$, the Green's function at the streamer location is computed.
- III The normal derivative of the Green's function at the streamer location can be obtained by taking the normal derivative of the result in (*II*). This is mathematically written as

$$\frac{\partial G(\mathbf{r_r})}{\partial n} = \frac{\partial G^0(\mathbf{r},\mathbf{r_r})}{\partial n} + \int_{S_{fs}} \frac{\partial G^0(\mathbf{r^s},\mathbf{r_r})}{\partial n} \frac{\partial G(\mathbf{r^s},\mathbf{r})}{\partial n_1} dS_{fs} \,. \quad (4)$$

SYNTHETIC DATA EXAMPLE

In this section we use synthetic data examples to investigate the performance of Eq. 2 for extracting the normal derivative of the pressure field. A 2D pressure field and its normal derivative were modeled using the integral method for a model consisting of rough sea surface and half space of water. The rough sea surface is based on a Pierson-Moskowitz spectrum (Pierson and Moskowitz, 1964) with a wind speed of 15 m/s. A source at 1 km depth and receivers at 7.5 m were used to compute the data. The data were generated using a temporal and spatial sampling of 4 ms and 6 m, respectively. Figures 3(a) and (b) show the modeled pressure field and its normal derivative, respectively. Their corresponding amplitude spectra are shown in Figs. 3(c) and (d). The amplitude spectra show that the receiver ghost notches are random; this is because the sea surface is very rough (having a root-mean-square wave height of 1.7 m). In order to better illustrate the behavior of the notches for rough sea, Figs. 4(a) and (b) show the amplitude and phase spectra of the ghost function calculated at vertical incidence, respectively. As a consequence of the rough sea surface, the following can be observed from these figures:

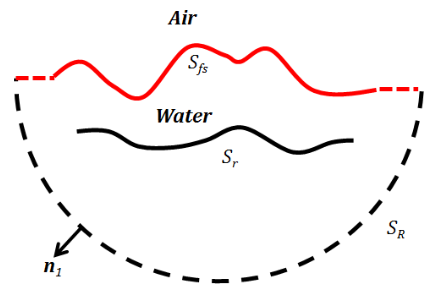

Figure 2: Problem geometry with the closed surface S comprising of the free surfaceS_{fs} and a hemispherical surface S_R.

- I Below 20 Hz the effect of rough sea is negligible.
- II The second notch location is different from a frequency location that would have been predicted by a flat sea surface.
- III The effect of incoherent scattering is stronger at higher frequencies.
- IV The signal level present at the notch location is small (or alternatively poor signal-to-noise ratio for field data). An attempt to deghost at this location would result in instability (or noise amplification for field data).
- V The phase of the ghost function undergoes a sharp change at the notch location, which is different from that predicted by a flat sea approximation.

Sea surface imaging was performed within a 1 s window following the event (cf. Fig. 3(a)) for different frequency bands (cf. Fig. 5). The imaged sea surfaces for the bandwidth $0-125$ Hz, $20-125$ Hz and $40-125$ Hz show very similar results. This is confirmed by comparing the results with the true sea surface. However, the effect of a band limited source wavefield and a limited aperture is still present. These negligible effects can easily be handled in practice.

The second step in the extraction of the pressure normal derivative is modeling of Green's functions and their corresponding normal derivatives (or the construction of the *monopole* and *dipole* matrices). Placing the Green's function source 10 m below the streamer, we generated the *monopole* and *dipole* matrices for Eq. 2. Here, the location of the Green's function source

DOI http://dx.doi.org/10.1190/segam2014-0480.1

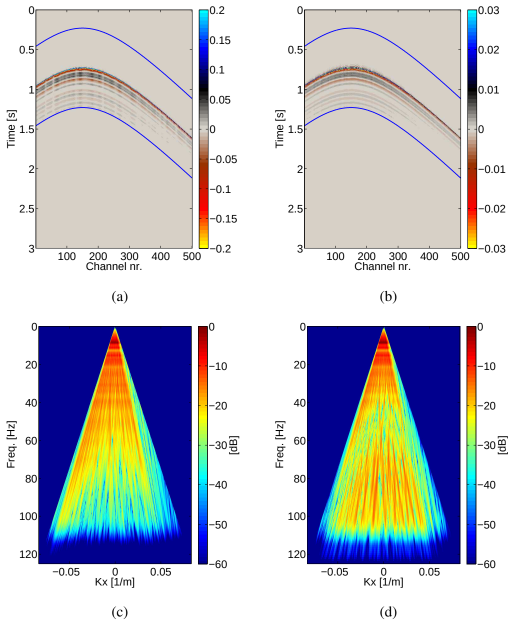

Figure 3: (a) Modeled presure wavefield, (b) the pressure normal derivative, (c) amplitude spectrum of (a), and (d) amplitude spectrum of (b).

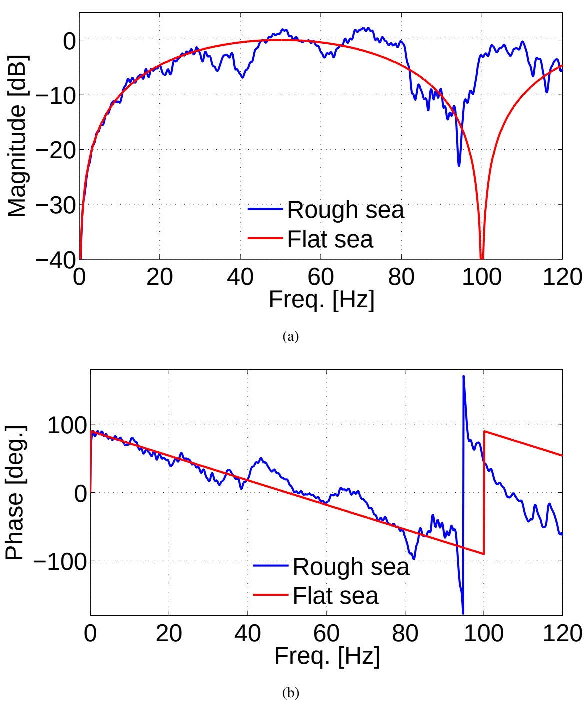

Figure 4: (a) Amplitude and (b) phase spectra of rough (blue) and flat (red) sea surface ghost functions at the vertical incidence.

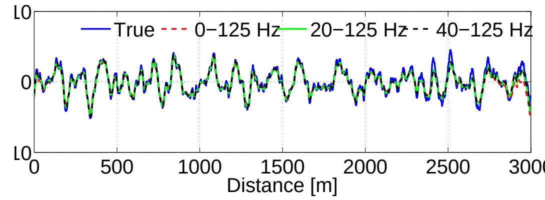

Figure 5: True and imaged sea surfaces obtained using different frequency bandwidths.

was selected after testing different locations and selecting that with the smallest artifact.

Finally, the normal derivative of the pressure field is extracted by solving an even-determined inverse problem based on Eq. 2. To avoid the receiver notch locations and possible instabilities associated with being close to the viccinity of these notches, the analysis was limited to the frequency band between 0 and 55 Hz. Firstly, assuming the sea surface shape is known exactly, we computed the residual between the modeled and extracted pressure normal derivative as shown in Fig. 6(a). This residual difference is negligible implying that the method correctly predicted the pressure normal derivative. Secondly, we used the imaged sea surface and again extracted pressure normal derivative and then computed the residual between the modeled and extracted pressure normal derivative as shown in Fig. 6(b)). Here, the residue is related to the negligible differences between the modeled and imaged sea surfaces.

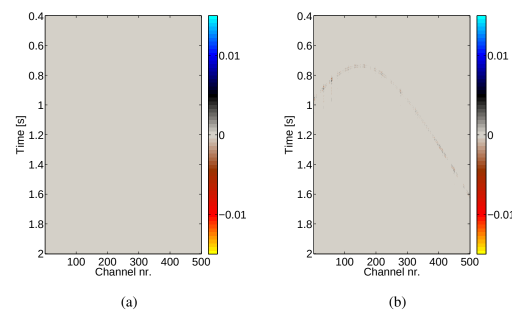

Figure 6: The residual between the modeled and extracted pressure normal derivative based on (a) Eq. 2, assuming the sea surface shape is known exactly, (b) using the imaged sea surface. NB: For the purpose of visualization, all the results are shown with half the color scale relative to that used for modeled pressure normal derivative data in Fig. 3(b).

FIELD DATA EXAMPLE

The field data was acquired by PGS using dual-sensor streamer in deep water offshore Brazil. Figures 7(a) and (b) respectively show a selected shot gather of the pressure wavefield and the associated amplitude spectrum. The notches in the amplitude spectrum are consistent with source and receiver depths of 7 m and 15 m respectively.

DOI http://dx.doi.org/10.1190/segam2014-0480.1

Sea surface imaging was performed using $20-25$ Hz high-pass filtered up- and down-going pressure wavefields within a 1 s window around the sea floor primary reflection event (cf. Fig. 7(a)). The peak to peak wave height estimated from the imaged sea surface is around 3.6 m, which matches the observers significant wave height estimate of $3.2-3.8$ m (cf. Fig. 8).

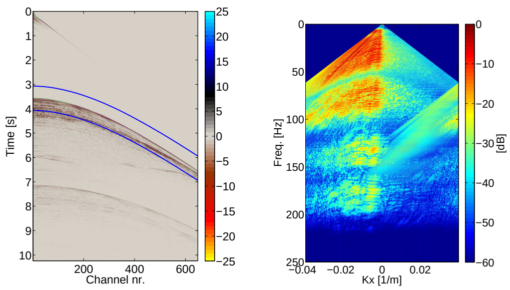

(a) (b)

Figure 7: (a) Presure wavefield and (b) its corresponding amplitude spectrum.

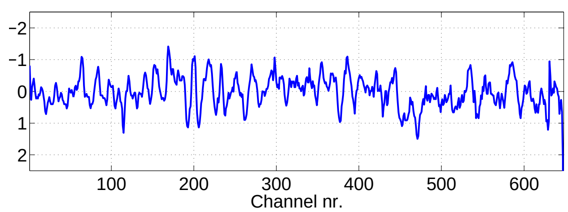

Figure 8: Imaged sea surface for the event following the primary reflection.

Employing the imaged sea surface and following the same approach as in the synthetic data section, the normal derivative of the pressure field was extracted. Since the data is from deep water, we utilized a 2D Green's function for the construction of the *monopole* and *dipole* matrices. Figures 9(a) and (b) respectively show the extracted pressure normal derivative and its amplitude spectrum for the time window following the primary reflection of the sea floor event. The validity of the results were confirmed by computing the residual between the extracted pressure normal derivative and the normal derivative of the pressure field obtained from the measured vertical particle velocity within the frequency band between 15 and 45 Hz (cf. Fig. 9(c)). The negligible residue confirm that the extraction of the normal derivative of the pressure field was successful. Nevertheless, the minor differences can be attributed to possible discrepancies between the imaged and the true sea surface as demonstrated using synthetic data.

CONCLUSION

A wave theoretical method based on Kirchhoff-Helmholtz integral equation for extracting the normal derivative of the pressure field at the recording surface for any arbitrarly shaped sea surface is proposed. The method requires the Green's function that contains the scattering information from the spatio-temporally varying sea surface. This is achieved by first imaging the sea surface employing dual sensor data for the frequency band with high signal-to-noise ratio (i.e. high frequencies) and then computing the Green's function utilizing the Kirchhoff-Helmholtz integral equation for a closed surface with an actual source that is a Dirac delta pulse in space. The validity of the technique has been examined using a rough sea synthetic data modeled using the integral method and deep water field data from offshore Brazil. In both tests a successful extraction of the normal derivative of the pressure field was obtained.

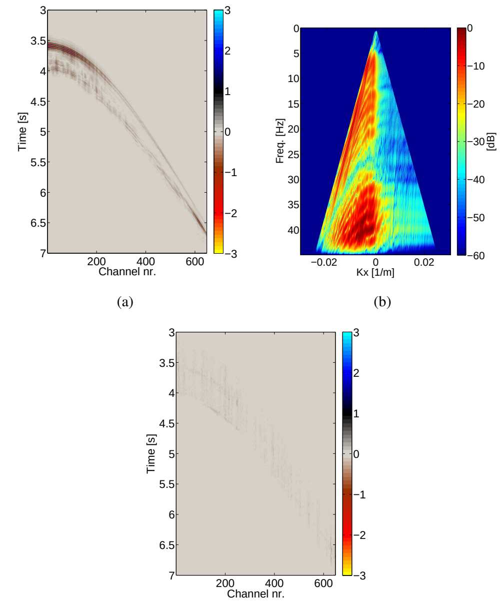

(a) (b) (c)

Figure 9: (a) Extracted pressure normal derivative for the primary event and (b) its corresponding amplitude spectrum. (c) The residual between the measured and extracted pressure normal derivatives.

ACKNOWLEDGMENTS

We thank PGS for permission to publish this work. We are grateful to our colleagues Hocine Tabti, Tilman Klüver and Anthony Day for fruitful dicussions.

http://dx.doi.org/10.1190/segam2014-0480.1

EDITED REFERENCES

Note: This reference list is a copy-edited version of the reference list submitted by the author. Reference lists for the 2014 SEG Technical Program Expanded Abstracts have been copy edited so that references provided with the online metadata for each paper will achieve a high degree of linking to cited sources that appear on the Web.

REFERENCES

Amundsen, L., 1994, The propagator matrix related to the Kirchhoff-Helmholtz integral in inverse wavefield extrapolation: Geophysics, **59**, 1902–1910, http://dx.doi.org/10.1190/1.1443577.

Amundsen, L., B. Secrest, and B. Arntsen, 1995, Extraction of the normal component of the particle velocity from marine pressure data: Geophysics, **60**, 212–222, http://dx.doi.org/10.1190/1.1443749.

Copley, L. G., 1968, Integral equation method for radiation from vibrating bodies: The Journal of the Acoustical Society of America, **41**, 807–816, http://dx.doi.org/10.1121/1.1910410.

Laws, R., and E. Kragh, 2006, Sea surface shape derivation above the seismic streamer: Geophysical Prospecting, **54**, no. 6, 817–828.

Morse, P. M., and H. Feshbach, 1953, Methods of theoretical physics: McGraw-Hill.

Orji, O., W. Söllner, and L. J. Gelius, 2010, Imaging the sea surface using a dual-sensor towed streamer: Geophysics, **75**, no. 6, V111–V118, http://dx.doi.org/10.1190/1.3496439.

Orji, O., W. Söllner, and L. J. Gelius, 2012, Effects of time-varying sea surface in marine seismic data: Geophysics, **77**, no. 3, P33–P43, http://dx.doi.org/10.1190/geo2011-0361.1.

Pierson, W. J. Jr., and L. Moskowitz, 1964, A proposed spectral form for full developed wind seas based on the similarity theory of S. A. Kitaigorodskii: Journal of Geophysical Research, **69**, no. 24, 5181–5190, http://dx.doi.org/10.1029/JZ069i024p05181.

Schenck, H., 1968, Improved integral formulation for acoustic radiation problems: The Journal of the Acoustical Society of America, **44**, no. 1, 41–58, http://dx.doi.org/10.1121/1.1911085.

Sommerfeld, A., 1954, Optics: Academic Press.

Veronesi, W. A., and J. D. Maynard, 1989, Digital holographic reconstruction of sources with arbitrarily shaped surfaces: The Journal of the Acoustical Society of America, **85**, no. 2, 588–598, http://dx.doi.org/10.1121/1.397583.